Supporting Information for

Synthesis and Application of a Quaternary Phosphonium Polymer Coagulant to Avoid *N*-Nitrosamine Formation

Teng Zeng[†], *Joseph J. Pignatello*[‡], *Russell Jingxian Li*[§], *William A. Mitch*[†,*]

[†]Department of Civil and Environmental Engineering, Stanford University, 473 Via Ortega, Stanford, California 94305, United States

[‡]Department of Environmental Sciences, The Connecticut Agricultural Experiment Station, 123 Huntington Street, P.O. Box 1106, New Haven, Connecticut 06504-1106, United States

[§]Department of Chemistry, Stanford University, 333 Campus Drive, Stanford, California 94305, United States

*Corresponding Author

William A. Mitch: Email: wamitch@stanford.edu, Phone: 650-725-9298, Fax: 650-723-3505

(Total 26 pages, 7 texts, 2 schemes, 3 tables, and 11 figures)

Table of Contents

S1. Chemicals and reagents S3

S2. Synthesis of N-based and P-based polymers (Schemes S1-S2)..... S5

S3. Characterization of N-based and P-based materials (Figures S1-S4) S8

S4. Product analysis of reactions of N-based and P-based precursors (Table S1 and Figure S5)..... S14

S5. Quantum chemical evaluation of nitrosation pathways (Table S2) S17

S6. Product analysis of reactions of DEA and DEP under extreme acid-nitrite conditions (Figures S6-S8) . S18

S7. Coagulation and NOC formation potential of three source waters (Table S3 and Figures S9-S11)..... S21

References..... S25

S1. Chemicals and reagents

All chemicals were of reagent-grade purity or higher and were used as received unless otherwise specified, including: acetic acid (HOAc; glacial, ≥99.7%), acetonitrile (ACN; 99.9%), acetone (99.9%), dichloromethane (DCM; >99.9%), methanol (MeOH; >99.9%), aluminum sulfate hydrate ($Al_2(SO_4)_3 \cdot xH_2O$; 98.0-102.0%), ammonium chloride (NH_4Cl; ≥99.5%), hydrochloric acid (HCl; ≥36.5-38.0%), sodium hypochlorite (NaOCl; 5.65-6% w/v active chlorine), sodium hydroxide (NaOH; >99%), sodium sulfate (Na_2SO_4; anhydrous, ≥99.0%), and sulfuric acid (95.0-98.0%) from Fisher Scientific; allyl chloride (99%), allylmagnesium chloride (2.0 M in tetrahydrofuran), ammonium acetate (≥99.0%, eluent additive for LC-MS), ammonium hydroxide (≥25% in H_2O, eluent additive for LC-MS), L-ascorbic acid (≥99.0%), boric acid (99.5%), diallyldimethylammonium chloride (DADMAC; ≥97.0%), diethylamine (DEA; purified by re-distillation, 99.5%), diethyl ether (anhydrous, ≥99.7%), diethylphosphine (DEP; 98%), dimethylamine (DMA; 40 wt% in H_2O), *N*,*N*-diethyl-*p*-phenylenediamine (DPD; 97%), formic acid (~98%, eluent additive for LC-MS), hexadecyltrimethylammonium bromide (CTAB; ≥99%), iodine (≥99.8%), mercuric chloride (≥99.5%), *N*-nitrosodiethylamine (NDEA; 99%), *N*-nitrosodimethylamine (NDMA; 99%), poly(vinyl sulfate) potassium salt (PVSK; potassium 22.0-27.0%), potassium iodide (≥99.0%), sodium bicarbonate (99.5-100.5%), sodium nitrite ($NaNO_2$; ≥99.0%), sodium phosphate dibasic dehydrate (≥99.0%), sodium phosphate monobasic (≥99.0%), sulfamic acid (≥99%), sulfanilamide (≥99%), tetrahydrofuran (THF; anhydrous, ≥99.9%), and *ortho*-toluidine blue (*o*-Tb; technical grade) from Sigma-Aldrich; ammonium persulfate (APS; 98%) and chlorodiethylphosphine (Cl-DEP; 95%) from Acros Organics; allyldiethylamine (ADEA; 95%), allyldimethylamine (ADMA; 98%), and 4,4'-azobis(4-cyanovaleric acid) (azo-CNV; 98%) from Pfaltz & Bauer; diethylphosphine oxide (DEPO; 95%) and chlorodiethylphosphine oxide (Cl-DEPO; 95%) from Alfa Aesar; dimethyl sulfoxide-d_6 (DMSO-d_6; 99.9 atom% D) and *N*-nitrosodimethylamine-d_6 (NDMA-d_6; ≥98%) from Cambridge Isotope Laboratories.

Working solutions of free chlorine (HOCl) were prepared fresh daily by diluting a predetermined amount of NaOCl stock solution with ultrapure water (resistivity ≥18.2 MΩ·cm, Millipore). The concentration of HOCl was standardized at 292 nm ($\varepsilon_{292nm}(OCl^-)$ = 362 $M^{-1} \cdot cm^{-1}$)[1] using an Agilent Cary 60 UV-Vis

spectrophotometer. Working solutions of preformed monochloramine (NH_2Cl) were prepared fresh daily by dissolving NH_4Cl in ultrapure water adjusted to pH 9, followed by dropwise addition of standardized HOCl to obtain a Cl:N molar ratio of 1:1.2. The concentration of NH_2Cl was determined by deconvoluting solution absorbance at 245 nm ($\varepsilon_{245nm}(NH_2Cl)$ = 445 M^{-1} cm^{-1}) and 295 nm ($\varepsilon_{295nm}(NHCl_2)$ = 14 M^{-1} cm^{-1})[2] as previously described.[3] Working solutions of synthesized polyDADEAC and polyDADEPC were prepared by wetting polymer solids with appropriate amounts of ultrapure water to give a final concentration of 0.1% as active ingredient. Working solutions of polyDADMACs were prepared by diluting polymer stock solutions containing solid contents in the range of 10-40% with appropriate amounts of ultrapure water to give a final concentration of 0.1% as active ingredient. When necessary, solutions and reagents were deoxygenated with N_2 prior to use. Air and moisture sensitive compounds were stored inside a N_2-filled glove box until use.

S2. Synthesis of N-based and P-based polymers (Schemes S1-S2)

Synthesis of poly(diallyldiethylphosphonium chloride) (polyDADEPC)

A three-step synthesis protocol adapted from previously published methods was used for the preparation of poly(diallyldiethylphosphonium chloride (polyDADEPC) (Scheme S1). In the first step, a 100 mL flame-dried, round-bottomed flask, fitted with a magnetic stir bar, a N_2 inlet tube, and air-tight septa, was flushed thoroughly with N_2. The flask was then charged with 9.7 mL (79.67 mmol) of chlorodiethylphosphine and 50 mL of anhydrous THF and cooled to -78 °C in a dry ice-acetone bath. To the resulting mixture was added, dropwise via a N_2-purged syringe, 40 mL of 2 M allylmagnesium chloride in THF (80.00 mmol). After complete addition, the reaction mixture exhibited a white precipitate in a pale gray solution. The heterogeneous mixture was allowed to warm to room temperature, stirred under N_2 for 2 h, and left immersed in a preheated oil bath at 200 °C. The intermediate tertiary phosphine product, allyldiethylphosphine, was recovered by fractional distillation under reduced pressure (68-70 °C at 150 mmHg), yielding 5.8 g (44.56 mmol, 56%) of a clear, colorless liquid.

In the second step, a 50 mL flame-dried round-bottomed flask fitted with a N_2 inlet tube and air-tight septa was purged thoroughly with N_2 and charged with 1.32 g (10.14 mmol) of freshly distilled ADEP and 13 mL of anhydrous diethyl ether. To the resulting mixture was added, all at once via a N_2-purged syringe, 0.9 mL (11.04 mmol) of allyl chloride. The reaction mixture was left to stand at 30 °C for 15 d. The precipitated product, diallyldiethylphosphonium chloride (DADEPC), was collected by vacuum filtration, washed with two 50 mL portions of anhydrous diethyl ether, and recovered by overnight evaporation of ether under high vacuum, yielding 0.58 g (2.81 mmol, 27%) of hygroscopic white needle-like crystals.

In the third step, a 10 mL flame-dried Pyrex vial was brought inside a N_2-filled glove box, flushed thoroughly with N_2 via pump-down cycles, and charged with 0.50 g (2.42 mmol) of DADEPC and 1 mL of N_2-purged ultrapure water. To the resulting solution was added, two weight percent (relative to the initial DADEPC mass) of 4,4’-azobis(4-cyanovaleric acid) (azo-CNV) as the free radical initiator. The reaction mixture was sealed and heated at 75 °C on a hotplate for 24 h. The solidified polymer product, polyDADEPC, was washed

with 50 mL of anhydrous diethyl ether and recovered by overnight evaporation of ether under high vacuum, yielding 0.42 g (84 wt% of the initial DADEPC mass) of a light yellow solid.

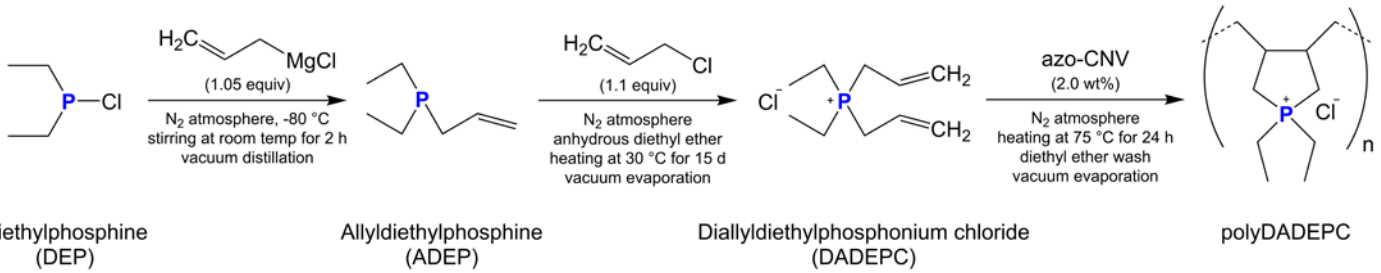

Scheme S1. Schematic of poly(diallyldiethylphosphonium chloride) (polyDADEPC) synthesis.

Synthesis of poly(diallyldiethylammonium chloride) (polyDADEAC)

A three-step synthesis protocol adapted from previously published methods was used for the preparation of poly(diallyldiethylammonium chloride) (polyDADEAC) (Scheme S2). In the first step, a 100 mL three-necked, round-bottomed flask, fitted with a magnetic stir bar, a thermometer, and two addition funnels, was charged with 8.3 mL (80.23 mmol) of DEA and 11 mL of ultrapure water. To the resulting solution was added alternately, dropwise via addition funnels, 6.8 mL (83.44 mmol) of allyl chloride and 8 mL (100.00 mmol) of 50% NaOH solution. After complete addition, the biphasic reaction mixture of an oily layer was stirred on a hotplate at 60 °C for 4 h. The intermediate tertiary amine product, allyldiethylamine (ADEA), was recovered by fractional distillation (110 °C at 760 mmHg) and dried over NaOH pellets for 24 h, yielding 6.8 g (60.07 mmol, 75%) of a clear, colorless liquid.

In the second step, a 50 mL oven-dried, round-bottomed flask was charged with 1.18 g (10.42 mmol) of freshly distilled ADEA and 11 mL of anhydrous acetone. To the resulting mixture was added, all at once via a N_2-purged syringe, 0.9 mL (11.04 mmol) of allyl chloride. The reaction mixture was left to stand at 30 °C for 7 d. The precipitated product, diallyldiethylammonium chloride (DADEAC), was collected by vacuum filtration, washed with two 50 mL portions of dry acetone, and recovered by overnight evaporation of acetone under high vacuum, yielding 1.24 g (6.56 mmol, 63%) of hygroscopic colorless crystals.

In the third step, a 10 mL oven-dried Pyrex vial was brought inside a N_2-filled glove box, flushed thoroughly with N_2 via pump-down cycles, and charged with 1.02 g (5.37 mmol) of DADEAC dissolved in 2 mL of N_2-purged ultrapure water. To the resulting solution was added, all at once, two weight percent (relative to the DADEAC mass) of ammonium persulfate (APS) as the free radical initiator. The reaction mixture was sealed and heated at 75 °C on a hotplate for 24 h. The solidified polymer product, poly(diallyldiethylammonium chloride) (polyDADEAC), was washed with 50 mL of anhydrous acetone and recovered by overnight evaporation of acetone under high vacuum, yielding 0.94 g (92 wt% of the initial DADEAC mass) of a light yellow solid.

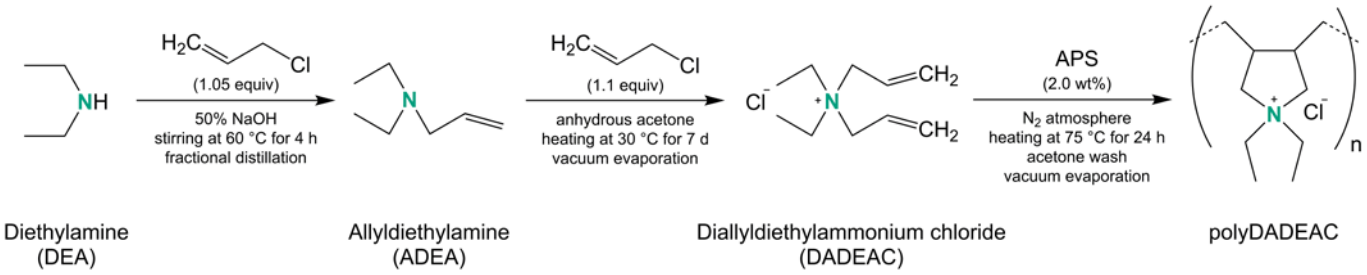

Scheme S2. Schematic of poly(diallyldiethylammonium chloride) (polyDADEAC) synthesis.

In the present study, allyl chloride was chosen over allyl bromide as the allylation reagent mainly for two reasons. First, bromide ion may suppress the cyclopolymerization process either by the scavenging of starting radical or by the termination of chain growth.[4] Second, bromide ion may interfere with the subsequent NOC formation potential tests by producing more reactive brominated oxidant species (e.g., bromochloramine) from reactions with chloramines, which is known to catalyze the formation of *N*-nitrosamines such as NDMA.[5,6]

S3. Characterization of N-based and P-based materials (Figures S1-S4)

^{31}P NMR spectra were acquired on a Varian Mercury Plus 400 MHz spectrometer equipped with a four-nucleus switchable and pulse field gradient probe operating at 162 MHz.[7] Samples were prepared in DMSO-d_6. Decoupled ^{31}P spectra were recorded at room temperature, using a 100 kHz spectral width, a 0.64 s acquisition time, a 4 s relaxation delay, 8 μs for a 55.4° pulse, and 1 Hz line broadening using 128 scans. ^{31}P chemical shifts were reported in parts per million (ppm) with reference to 85% H_3PO_4 (0.0 ppm). Instrument control and data acquisition were performed using the Varian *VNMR* software.

Accurate masses were measured on an Agilent 1260 Infinity high-performance liquid chromatography system interfaced to an Agilent 6520 Accurate-Mass quadrupole-time-of-flight (QToF) mass spectrometer equipped with a dual electrospray ionization source (ESI) (LC-ESI-QToF-MS).[8] Chromatographic separation was achieved on a Phenomenex Gemini-NX C18 column (100 × 2 mm, 5 μm) using a mobile phase of ultrapure water (with 0.1% v/v formic acid) and acetonitrile (with 0.1% v/v formic acid). A 17-min gradient elution at a flow rate of 0.4 mL/min was used: 3% acetonitrile for 2 min, 3–97% over 8 min, 97% for 2 min, 97–3% over 1 min, 3% for 0.5 min, 3–97% over 1 min, 97% for 0.5 min, 97–3% over 1 min, and 3% for 1 min. Electrospray ionization was performed in positive ion mode using the following parameters: capillary voltage 3500 V, nebulizer pressure 25 psi, drying gas temperature 300 °C, drying gas flow 10 L/min, fragmentor voltage 100 V, skimmer voltage 65 V, octopole 1 RF Vpp 750 V. High-resolution MS scans were acquired over a mass range from *m/z* 50 to 1700 at 1.41 spectra/s and 709.2 ms/spectrum. A reference mass solution containing *m/z* 121.050873 and 922.009798 was continuously introduced into the MS system to ensure a mass accuracy of <0.2 ppm over the mass range. Instrument control and data acquisition were performed using the Agilent *MassHunter* software.

Elemental analyses were conducted by ALS Environmental, Inc. (Tucson, AZ). Carbon, hydrogen, and nitrogen contents were determined by dry combustion and subsequent measurement of evolved gaseous products by infrared absorption following ASTM Method D5373-08. Phosphorus content was determined by

microwave-assisted acid digestion and subsequent measurement of acid-digested products by inductively coupled plasma-optical emission spectrometry following EPA Method 3052/6010C.

Molecular weights were measured on a Shimadzu size exclusion chromatography (SEC) system consisting of an LC-20AD liquid chromatography system interfaced to a RID-10A refractive index detector.[7] Chromatographic separation was achieved on a Sepax SRT SEC-500 analytical column (300 × 7.8 mm, 5 μm, 500 Å) using a mobile phase of sodium phosphate buffer (150 mM, pH 7). The column temperature was maintained at 40 °C in a thermostatted column oven. A 15-min isocratic elution at a flow rate of 1.0 mL/min was used. The MWs of polymers were calibrated with two sets of poly(ethylene glycol) (PEG) and poly(ethylene oxide) (PEO) standards of known peak molecular weights (M_p) obtained from Agilent (M_p 4.0–1522 kDa) and Fluka (M_p 6.7–1015 kDa). Instrument control and data acquisition were performed using the Shimadzu *LCsolution* software.

Charge densities were determined by the colloid titration method[9,10] using poly(vinyl sulfate) potassium salt (PVSK) as the standard anionic titrant.[11] The charge density of PVSK was standardized against a cationic surfactant hexadecyltrimethylammonium bromide with a known charge density of 2.7 meq/g. A definite amount of polymer sample diluted in ultrapure water (adjusted to pH 5, 7, or 9 with 0.01 N NaOH/HCl) was titrated against PVSK using *ortho*-toluidine blue (*o*-Tb) as a color indicator. Titration was monitored as the reduction in absorbance at 635 nm using an Agilent Cary 60 UV-Vis spectrophotometer until the sharp color change of *o*-Tb from blue to red-violet. The CDs of polymers were derived from the inflection points (i.e., equivalence points) of PVSK titration curves.[12] Data analysis was performed using the GraphPad *Prism* software.

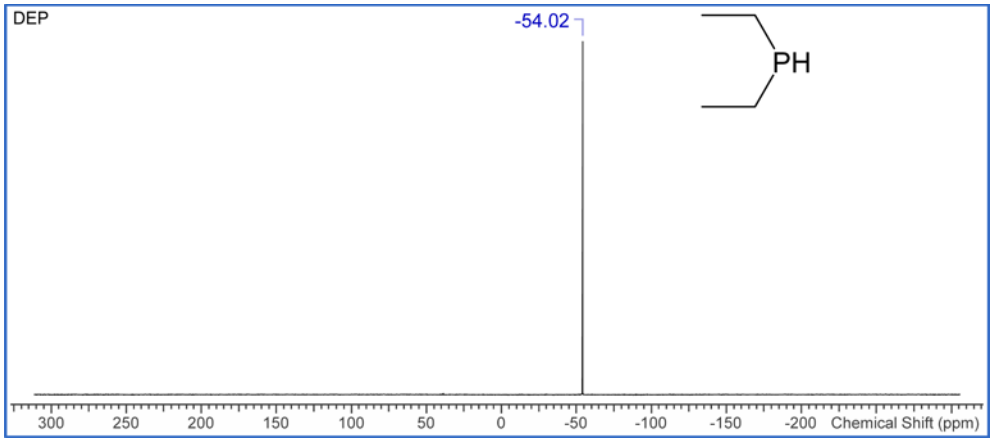
DEP
-54.02
PH
300 250 200 150 100 50 0 -50 -100 -150 -200 Chemical Shift (ppm)

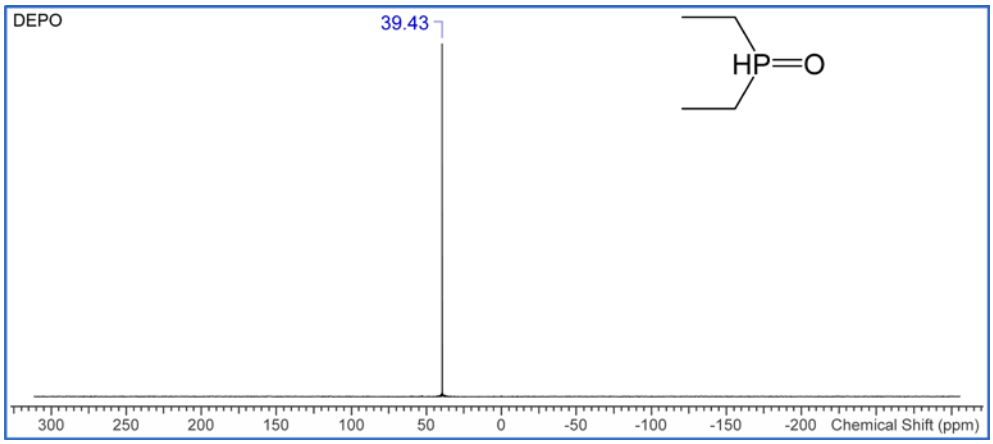
DEPO
39.43
HP=O
300 250 200 150 100 50 0 -50 -100 -150 -200 Chemical Shift (ppm)

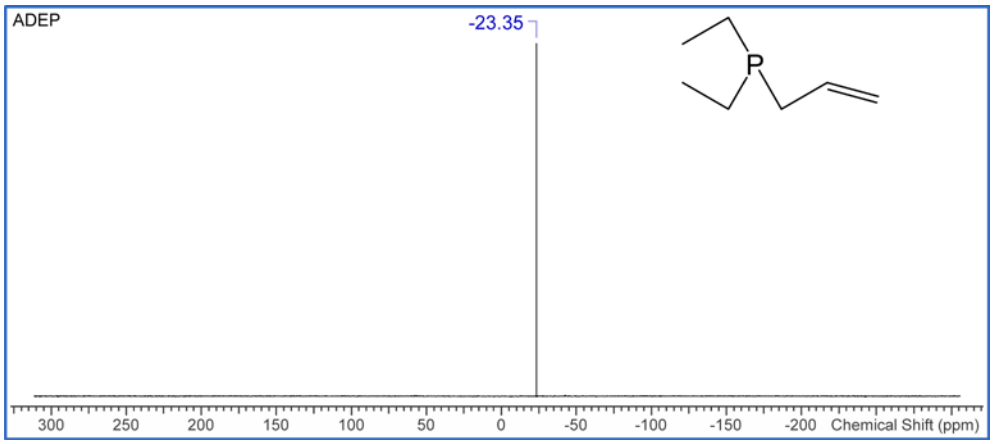
ADEP
-23.35
P
300 250 200 150 100 50 0 -50 -100 -150 -200 Chemical Shift (ppm)

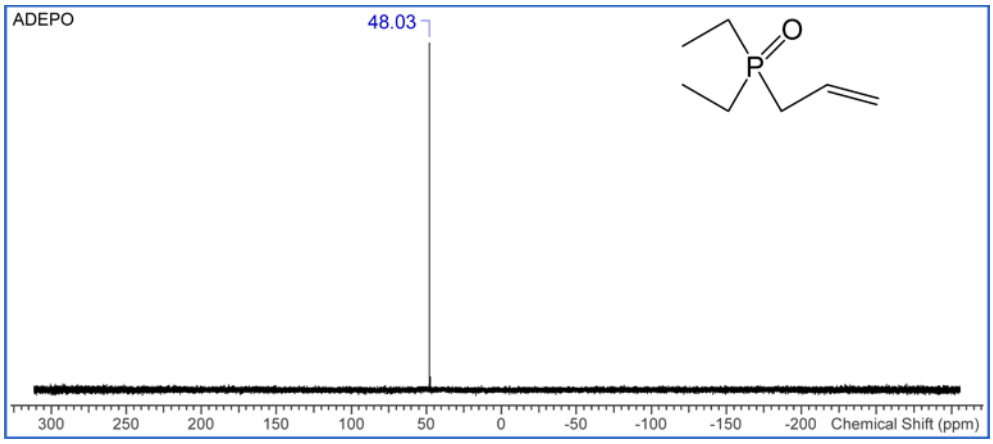
ADEPO
48.03
O
P
300 250 200 150 100 50 0 -50 -100 -150 -200 Chemical Shift (ppm)

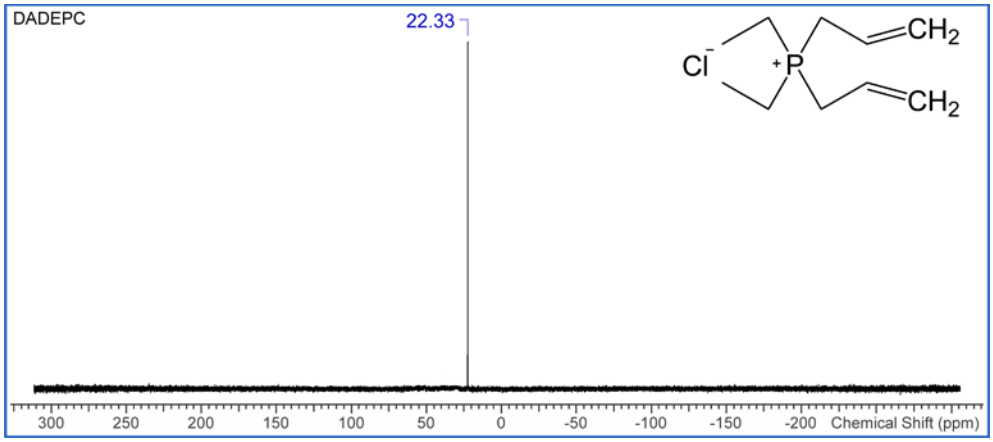

Figure S1. ^{31}P NMR spectra of (a) diethylphosphine (DEP), (b) diethylphosphine oxide (DEPO), (c) allyldiethylphosphine (ADEP), (d) allyldiethylphosphine oxide (ADEPO), and (e) diallyldiethylphosphonium chloride (DADEPC).

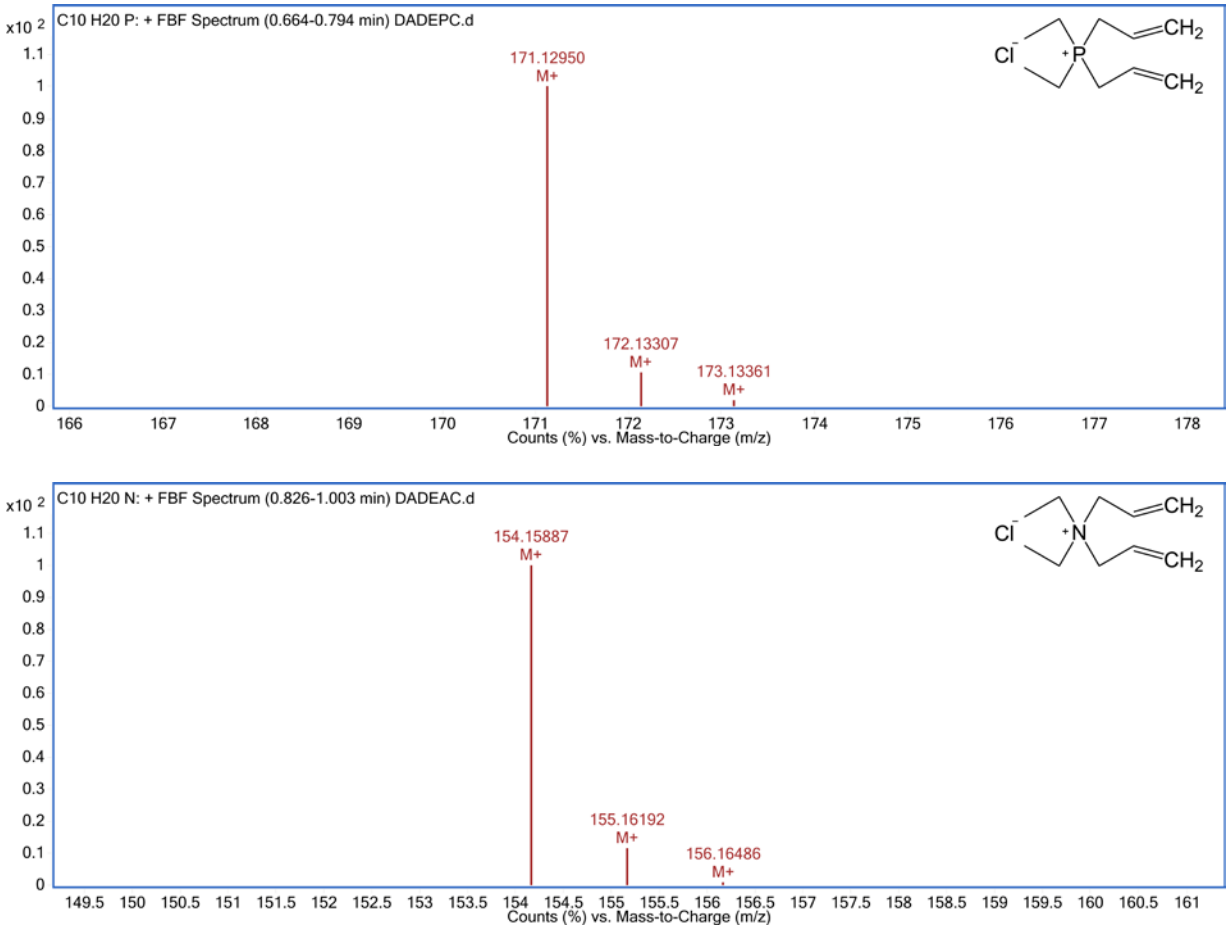

Figure S2. High-resolution mass spectra of (a) diallyldiethylphosphonium chloride (DADEPC) and (b) diallyldiethylammonium chloride (DADEAC).

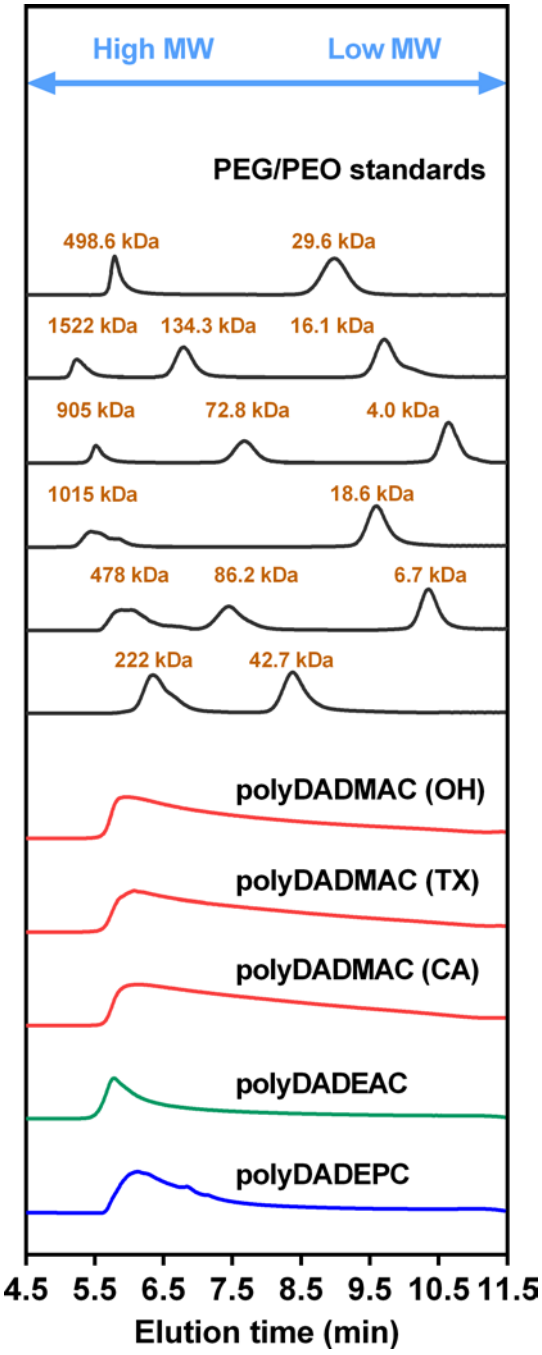

Figure S3. Size exclusion chromatograms of poly(ethylene glycol) (PEG) and poly(ethylene oxide) (PEO) standards, three commercial polyDADMACs, and synthesized polyDADEAC and polyDADEPC.

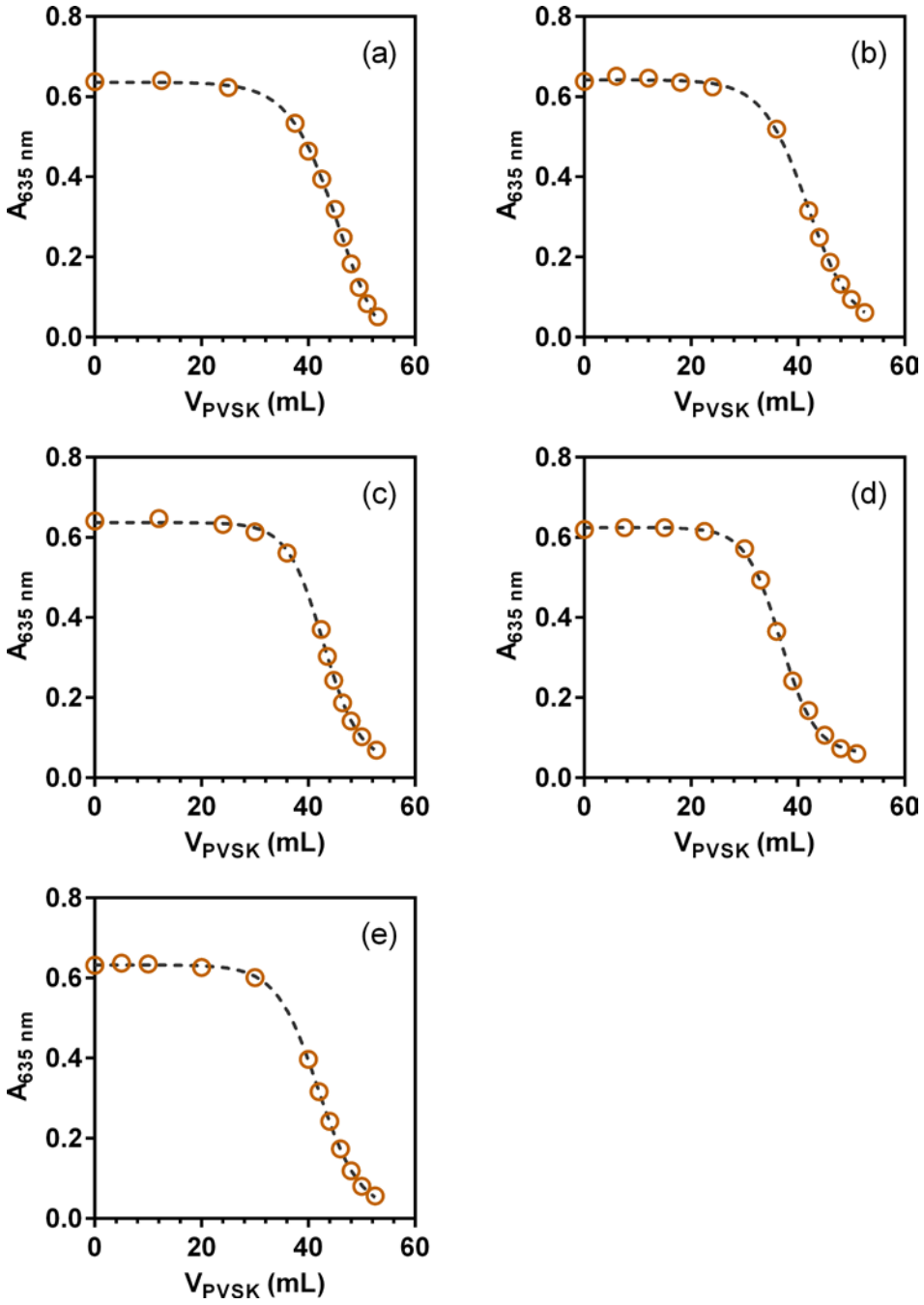

Figure S4. Poly(vinyl sulfate) potassium salt (PVSK) titration curves (at pH 7) of (a) polyDADMAC (OH), (b) polyDADMAC (TX), (c) polyDADMAC (CA), (d) polyDADEC, and (e) polyDADEPC. Dash lines represent logistic dose-response fits to the data. The $\log IC_{50}$ values, corresponding to the upper inflection points of titration curves, were used for the calculation of charge densities.

S4. Product analysis of reactions of N-based and P-based precursors (Table S1 and Figure S5)

Specific *N*-nitrosamines (i.e., NDMA and *N*-nitrosodiethylamine (NDEA)) as well as major oxygenated phosphine products (i.e., diethylphosphine oxide (DEPO), diethylphosphinic acid (DEPA), and allyldiethylphosphine oxide (ADEPO)) were analyzed on an Agilent 1260 Infinity high-performance liquid chromatography system interfaced to an Agilent 6460 triple quadrupole (QqQ) mass spectrometer equipped with an AJS electrospray ionization source (ESI) (LC-ESI-QqQ-MS/MS). Chromatographic separation was achieved on an Agilent Poroshell 120 EC-C18 column (50 × 2.1 mm, 2.7 µm) using a mobile phase of ammonium acetate (5 mM) and acetonitrile. The column temperature was maintained at 30 °C in a thermostatted column compartment. A 15-min gradient elution at a flow rate of 0.2 mL/min was applied: 5% acetonitrile for 1 min, 5–100% over 5 min, 100% for 1 min, 100–5% over 1 min, and 5% for 7 min. Electrospray ionization was performed in positive ion mode using the following parameters: capillary voltage 3500 V, nozzle voltage 500 V, nebulizer pressure 45 psi, drying gas temperature 300 °C, drying gas flow 5 L/min, sheath gas temperature 250 °C, and sheath gas flow 7 L/min. MS data were acquired in the multiple reaction monitoring (MRM) mode using one principal MRM transition for quantitation and one additional transition to serve as a qualifier for each analyte. Instrument control and data acquisition were performed using the Agilent *MassHunter* software.

Table S1. Optimized multiple reaction monitoring (MRM) transitions for N-based and P-based product analysis

Compound	MRM[a] (quantitation) (qualifier)	Precursor ion	Product ions	Fragmentor (V)	CE (V)	CAV (V)
NDMA	75 → 43	75	43 $[M + H - NHOH]^+$	99	15	2
	75 → 58	$[M + H]^+$	58 $[M + H - OH]^+$			
NDEA	103 → 75	103	75 $[M + H - C_2H_4]^+$	97	8	6
	103 → 47	$[M + H]^+$	47 $[M + H - C_2H_4 - C_2H_4]^+$			
DEPO	107 → 61	107	61 $[M + H - C_2H_5 - OH]^+$	135	18	5
	107 → 79	$[M + H]^+$	79 $[M + H - C_2H_2]^+$			
DEPA	123 → 77	123	77 $[M + H - C_2H_5 - OH]^+$	135	25	6
	123 → 105	$[M + H]^+$	105 $[M + H - OH]^+$			
ADEPO	147 → 77	147	77 $[M + H - C_2H_5 - C_3H_5]^+$	135	21	4
	147 → 61	$[M + H]^+$	61 $[M + H - C_2H_2 - C_3H_5 - OH]^+$			
DADEPC	171 → 102	171	102 $[M - C_3H_6 - C_2H_4]^+$	135	19	5
	171 → 129	$[M]^+$	129 $[M - C_3H_6]^+$			

[a] Primary transition and secondary transition were used for quantitation and confirmation, respectively. [b] Collision energy. [c] Cell accelerator voltage.

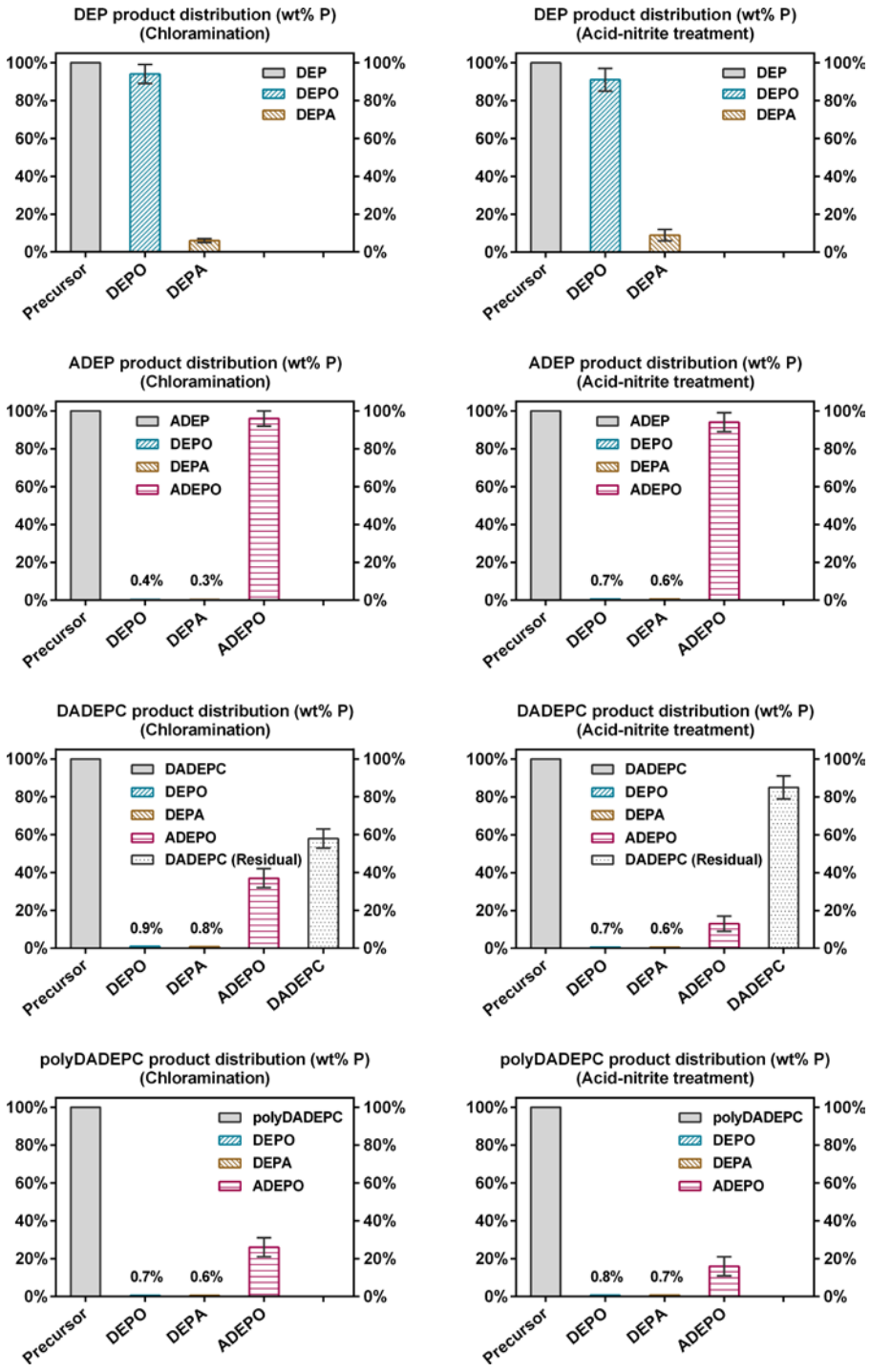

Figure S5. Observed product yields of P-based precursors diethylphosphine (DEP), allyldiethylphosphine (ADEP), diallyldiethylphosphonium chloride (DADEPC), and poly(diallyldiethylphosphonium chloride) (polyDADEPC) upon chloramination or acid-nitrite treatment. Identified products included diethylphosphine oxide (DEPO; observed mass = 106.05477, theoretical mass = 106.05475, error = 0.21 ppm, matching score = 99.98), diethylphosphinic acid (DEPA; observed mass = 122.04959, theoretical mass = 122.04967, error = -0.66 ppm, matching score = 99.85), and allyldiethylphosphine oxide (ADEPO; observed mass = 146.08599, theoretical mass = 146.08605, error = -0.42 ppm, matching score = 99.47). Error bars represent the range of duplicate measurements.

S5. Quantum chemical evaluation of nitrosation pathways (Table S2)

All quantum chemical calculations were performed using *Gaussian 09* (*revision C.01*, Gaussian Inc.)[13] available through the Stanford University Research Computing. Full geometry optimizations of reactants and products were performed using Becke's three-parameter hybrid functional[14] with Lee-Yang-Parr's gradient corrected correlation functional[15] (B3LYP) in conjunction with the 6-311+G(d,p) basis set[16] without symmetry constraints. Vibrational frequencies were calculated to verify that a given structure represented a minimum on the potential energy surface (i.e., no imaginary frequencies). Because the reactions occurred in aqueous phase, the solvent effect was taken into account using the conductor-like polarizable continuum model (CPCM),[17] with a dielectric constant of 78.39 for water.[18] Single-point energies were calculated on the basis of optimized geometries at the B3LYP / 6-311+G(d,p) level using the CCSD(T)[19] method in conjunction with the 6-311+G(d,p) basis set at 298.15 K and 1 atm. The Gibbs free energies of reaction (ΔG_r) were calculated to compare the relative thermodynamic favorability of amine and phosphine nitrosation and oxidation pathways.

Table S2. Calculated ΔG_r for nitrosation and oxidation reactions of DMA, DEA, and DEP

	Reaction	$\Delta G_{r,(aq)}$ (kcal/mol)[a]
	Nitrosation (chloramination)	
(1)	DMA + $NHCl_2$ + O_2 → NDMA + HCl + HOCl	-40.62
(2)	DEA + $NHCl_2$ + O_2 → NDEA + HCl + HOCl	-38.82
(3)	DEP + $NHCl_2$ + O_2 → NDEP + HCl + HOCl	-32.01
	Nitrosation (acid-nitrite treatment)	
(4)	DMA + N_2O_3 → NDMA + HNO_2	-39.96
(5)	DEA + N_2O_3 → NDEA + HNO_2	-38.16
(6)	DEP + N_2O_3 → NDEP + HNO_2	-31.36
	Oxidation	
(7)	DMA + ½ O_2 → DMHA (*N*-dimethylhydroxylamine)	5.11
(8)	DEA + ½ O_2 → DEHA (*N*-diethylhydroxylamine)	10.38
(9)	DEP + ½ O_2 → DEPO	-50.87
(10)	DEP + O_2 → DEPA	-104.96

[a] As a well-defined approximation for reactions in aqueous phase,[20] thermal corrections to Gibbs free energies calculated at the B3LYP / 6-311+G(d,p) level were used to correct single-point energies of reactants and products calculated at the CPCM-CCSD(T) / 6-311+G(d,p) // B3LYP / 6-311+G(d,p) level.

S6. Product analysis of reactions of DEA and DEP under extreme acid-nitrite conditions (Figures S6-S8)

Attempts were made to synthesize *P*-nitrosodiethylphosphine (NDEP) from neat diethylphosphine (DEP) under oxygen-free, extreme acid-nitrite conditions following an identical synthetic route for *N*-nitrosodiethylamine (NDEA).

A 20 mL oven-dried Pyrex vial was charged with 1.0 g (13.67 mmol) of diethylamine (DEA) and 10 mL of HOAc. To the resulting solution was added, dropwise via a glass pipette, 5 mL of 5 M $NaNO_2$ solution under rapid stirring. After complete addition, the bright yellow reaction mixture was allowed to cool to room temperature and stirred for 2 h. The resulting solution was combined with 15 mL of ultrapure water and extracted with five 20 mL portions of DCM. All DCM extracts were combined and dried over anhydrous Na_2SO_4 overnight. The product, *N*-nitrosodiethylamine (NDEA), was recovered by rotary evaporation of DCM, yielding 1.38 g (13.53 mmol, 99%) of yellow solids.

A 24 mL oven-dried Pyrex vial was brought inside a N_2-filled glove box, flushed thoroughly with N_2 via three pump-down cycles, and charged with 1.0 g (9.43 mmol) of diethylphosphine (DEP) and 10 mL of N_2-purged acetic acid. To the resulting solution was added, dropwise via a glass pipette, 5 mL of 5 M N_2-purged $NaNO_2$ solution under rapid stirring. After complete addition, the bright yellow reaction mixture was allowed to cool to room temperature and stirred overnight. The resulting solution was combined with 15 mL of N_2-purged ultrapure water and extracted with five 20 mL portions of DCM outside the glove box. All DCM extracts were combined and dried over anhydrous Na_2SO_4 overnight. The product was recovered by rotary evaporation of DCM, yielding 1.02 g of a viscous, colorless liquid. The product was analyzed by ^{31}P NMR and HRMS as described in Section S3.

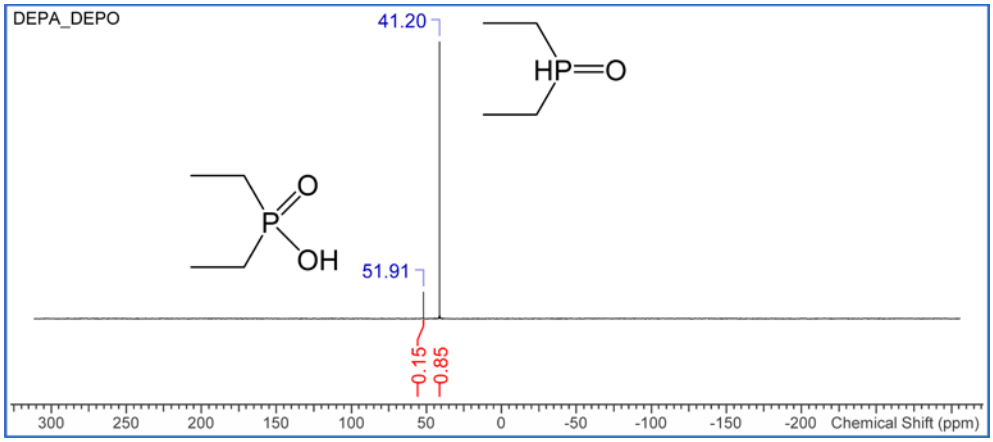

Figure S6. ^{31}P NMR spectrum of the nitrosation product mixture of diethylphosphine (DEP). The resonance at 41.2 ppm corresponds to diethylphosphine oxide (DEPO), while the resonance at 51.9 ppm corresponds to diethylphosphinic acid (DEPA).

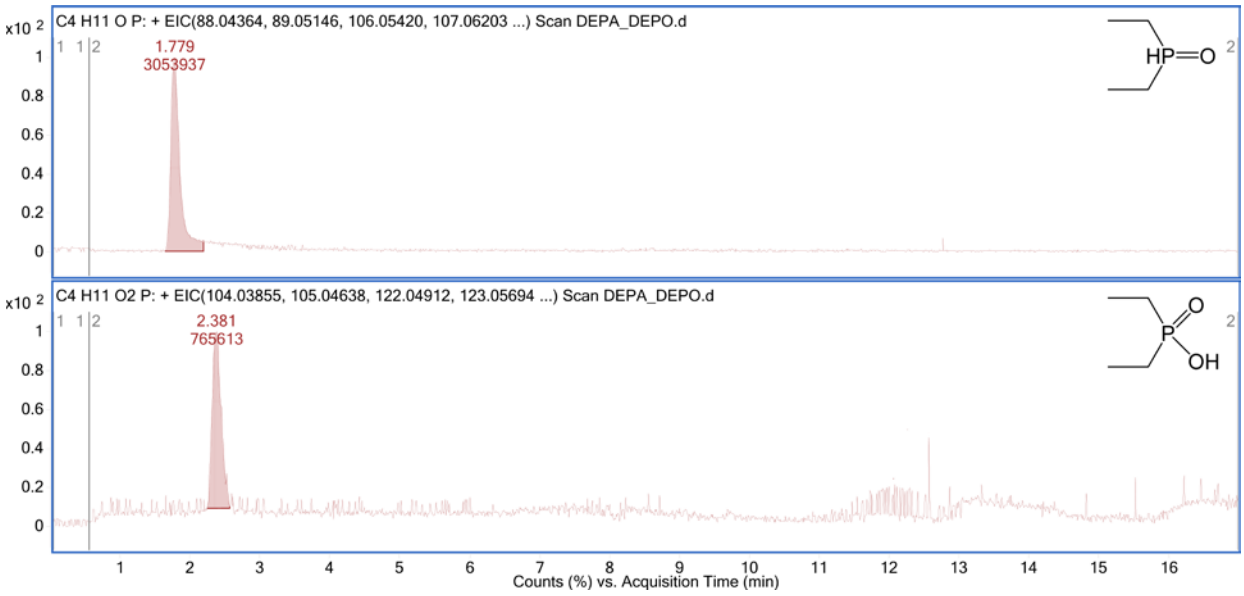

Figure S7. Extracted ion chromatograms of the nitrosation product mixture of diethylphosphine (DEP). The peak at 1.78 min corresponds to diethylphosphine oxide (DEPO), while the peak at 2.38 min corresponds to diethylphosphinic acid (DEPA).

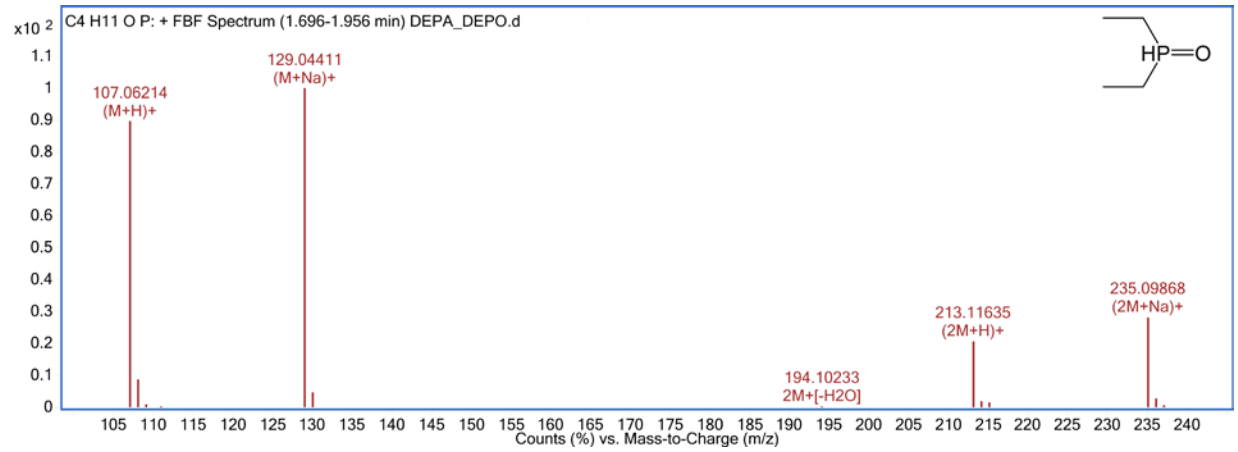

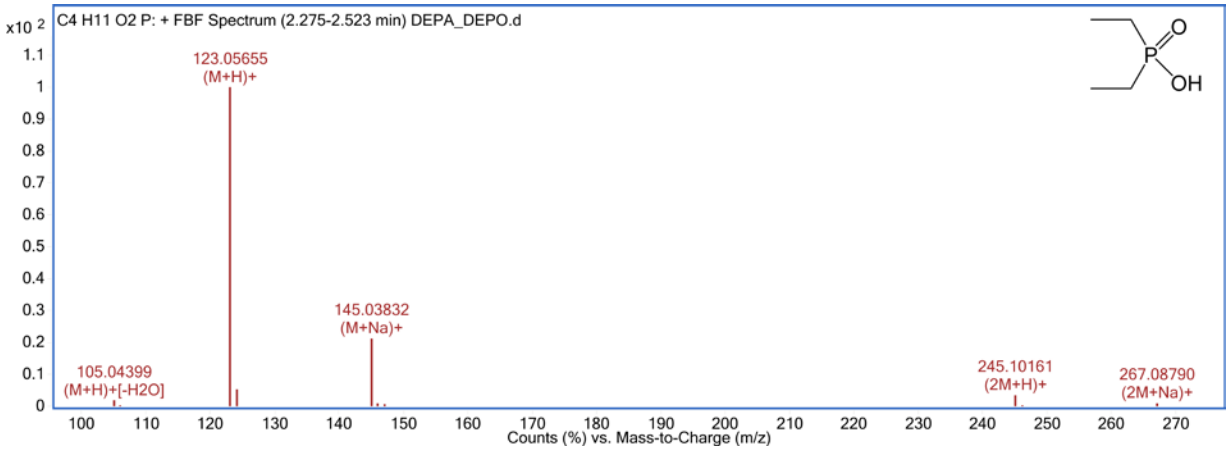

Figure S8. High-resolution mass spectra of diethylphosphine oxide (DEPO; observed mass = 106.05483, theoretical mass = 106.05475, error = 0.73 ppm, matching score = 99.84) and diethylphosphinic acid (DEPA; observed mass = 122.04913, theoretical mass = 122.04967, error = -4.43 ppm, matching score = 98.43) identified in the nitrosation product mixture of DEP.

S7. Coagulation and NOC formation potential of three source waters (Table S3 and Figures S9-S11)

Upon arrival, raw water samples were analyzed for a suite of water quality parameters: pH was measured using a Fisher Scientific Accumet Basic AB15 pH meter. Turbidity was measured using an HF Scientific DRT-15CE portable turbidimeter. Dissolved organic carbon (DOC) and total dissolved nitrogen (TDN) were measured using a Shimadzu TOC-L CPH total organic carbon analyzer (high temperature combustion at 720 °C; non-dispersive infrared detection) with a TNM-L total nitrogen unit (chemiluminescence detection). Dissolved inorganic nitrogen (DIN, equivalent to the sum of ammonium, nitrate, and nitrite) and dissolved inorganic phosphorus (DIP; equivalent to orthophosphate) were determined colorimetrically using a WestCo SmartChem 200 discrete analyzer. Dissolved organic nitrogen (DON) was calculated as the difference between TDN and DIN. Total dissolved phosphorus (TDP) was determined after acid-persulfate digestion using a Thermo Scientific iCAP 6300 ICP-OES CID spectrometer. Dissolved organic phosphorus (DOP) was calculated as the difference between TDP and DIP. Ultraviolet absorbance at 254 nm (UV_{254}) was measured using an Agilent Cary 60 UV-Vis spectrophotometer. Bromide and chloride were measured using a Dionex ICS-5000 ion chromatograph.

Bench-scale jar tests were conducted using a Yost & Son jar test apparatus following standard protocols currently practiced in participating utilities. For water OH, the water sample (1 L) was rapidly mixed for 30 s at 270 rpm before the addition of coagulants. Aluminum sulfate (17.5 mg/L) was added directly above and to the side of the stirring paddles and mixed for 8 s and then polymer (varying doses) was added and mixed for 13 s. Flash mix was followed by three slow mix stages, each at 65, 40, and 26 rpm for 12 min and 43 s. For water TX, the water sample was rapidly mixed for 30 s at 300 rpm before the addition of coagulants. Ferric chloride (8.7 mg/L) was added and mixed for 8 s and then polymer was added and mixed for 37 s. Flash mix was followed by two slow mix stages, one at 45 rpm for 1.5 min and the other at 30 rpm for 15 min. For water CA, the water sample was rapidly mixed for 30 s at 150 rpm before the addition of coagulants. Aluminum sulfate (7.5 mg/L) was added first and mixed for 8 s and then polymer was added and mixed for 52 s. Flash mix was followed by slow mix at 50 rpm for 15 min.

Specific *N*-nitrosamines were quantified following a modified EPA Method 521 protocol. Briefly, quenched samples were spiked with 20 ng/L of deuterated NDMA (NDMA-d_6) as an internal standard and passed through pre-conditioned UCT Enviro-Clean coconut shell-based activated carbon cartridges under an applied vacuum. Retained *N*-nitrosamines were eluted with dichloromethane (DCM). The DCM extracts were further dried over anhydrous Na_2SO_4 and concentrated to a final volume of ~1 mL under N_2. *N*-Nitrosamines were analyzed on an Agilent 7890A gas chromatography system interfaced to an Agilent 240 Ion Trap (IT) mass spectrometer in chemical ionization (CI) mode using liquid methanol as the reagent (GC-CI-IT-MS/MS). Chromatographic separation was achieved on a DB-1701 fused silica capillary column (20 m × 0.25 mm i.d. × 1 μm film thickness). Helium at a constant flow rate of 1.0 mL/min was used as the carrier gas. DCM extracts were injected in programmed temperature vaporization (PTV) solvent vent mode. A 35.5-min oven temperature gradient was used: 37 °C for 5 min, 4 °C/min to 130 °C, 10 °C/min to 160 °C, 40 °C/min to 250 °C, and 250 °C for 2 min. Chemical ionization was performed in positive ion mode using the following parameters: scan time 0.7 s, emission current 50 μA, solvent delay 9.5 min, transfer line temperature 230 °C, manifold temperature 80 °C, and ion trap temperature 150 °C. MS data were acquired in the MS/MS scan mode using one principal transition for quantitation and one additional transition to serve as a qualifier for each analyte. Instrument control and data acquisition were performed with the Agilent *WorkStation* software.

Total NOCs (TONO) were quantified following a protocol modified based on a method developed in our lab.[21] Briefly, a 500-mL sample was amended with sulfamic acid, incubated overnight, and passed through pre-conditioned activated carbon cartridges. Retained NOCs were sequentially eluted with DCM and MeOH. The DCM extracts were dried over anhydrous Na_2SO_4 and solvent-exchanged into MeOH. The combined MeOH extracts were further concentrated to a final volume of ~0.5 mL under N_2, treated with mercuric chloride and sulfanilamide, and injected into a heated reaction chamber containing tri-iodide-based reducing solution. Nitric oxide liberated from NOCs was continuously purged into an EcoPhysics CLD 88Yp chemiluminescence detector for analysis. The TONO signal responses were calibrated with reference to NDMA.

Table S3. Physicochemical properties of source waters

Parameter	Water OH	Water TX	Water CA
pH	7.4	8.0	7.6
Initial turbidity (NTU)	16.5	59.7	28.3
DOC (mgC/L)[a]	2.48 (±0.09)	7.47 (±0.09)	7.90 (±0.22)
UV_{254}	0.0644	0.2136	0.1093
$SUVA_{254}$ (L/mgC-m)	2.60	2.86	1.38
TDN (mgN/L)[a]	2.40 (±0.09)	2.78 (±0.20)	2.83 (±0.23)
NH_4^+ (mgN/L)[a]	0.12 (±0.03)	0.07 (±0.03)	0.05 (±0.03)
NO_2^- (mgN/L)	<0.02	<0.02	<0.02
NO_3^- (mgN/L)[a]	0.90 (±0.05)	0.41 (±0.05)	0.10 (±0.05)
DON (mgN/L)[b]	1.36 (±0.07)	2.28 (±0.19)	2.66 (±0.22)
TDP (mgP/L)[a]	0.03 (±0.02)	0.06 (±0.02)	0.05 (±0.02)
PO_4^{3-} (mgP/L)	0.02 (±0.01)	0.05 (±0.01)	0.04 (±0.01)
DOP (mgP/L)	<0.01	<0.01	<0.01
Br^- (µg/L)	37.8	96.6	415.2
Cl^- (mg/L)	4.0	69.6	21.2

[a] Errors represent one standard deviation from triplicate measurements. [b] Errors represent propagation through "TDN" minus "$NH_4^+ + NO_2^- + NO_3^-$".

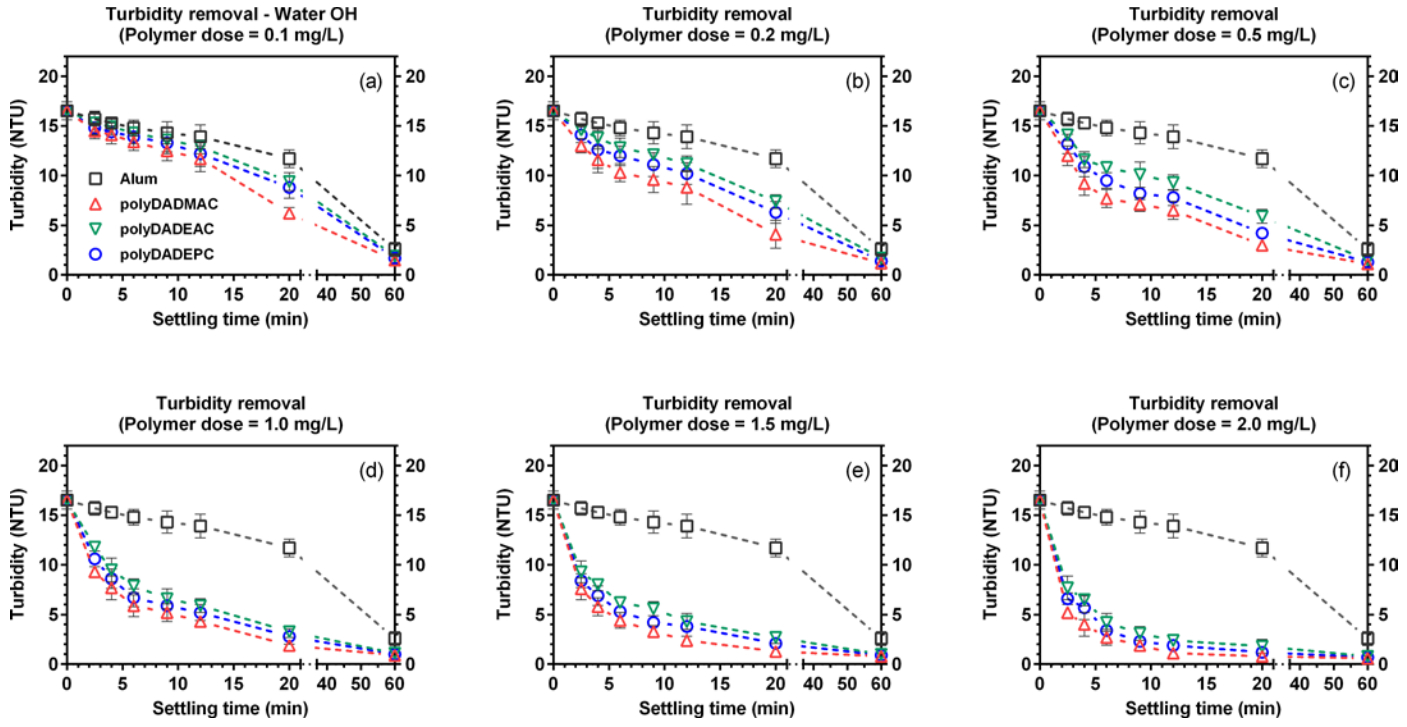

Figure S9. Time courses of turbidity removal at varying polymer doses in water OH. "Alum" indicates that only aluminum sulfate was dosed to serve as a benchmark. Error bars represent the range of duplicate measurements; where absent, bars fall within symbols.

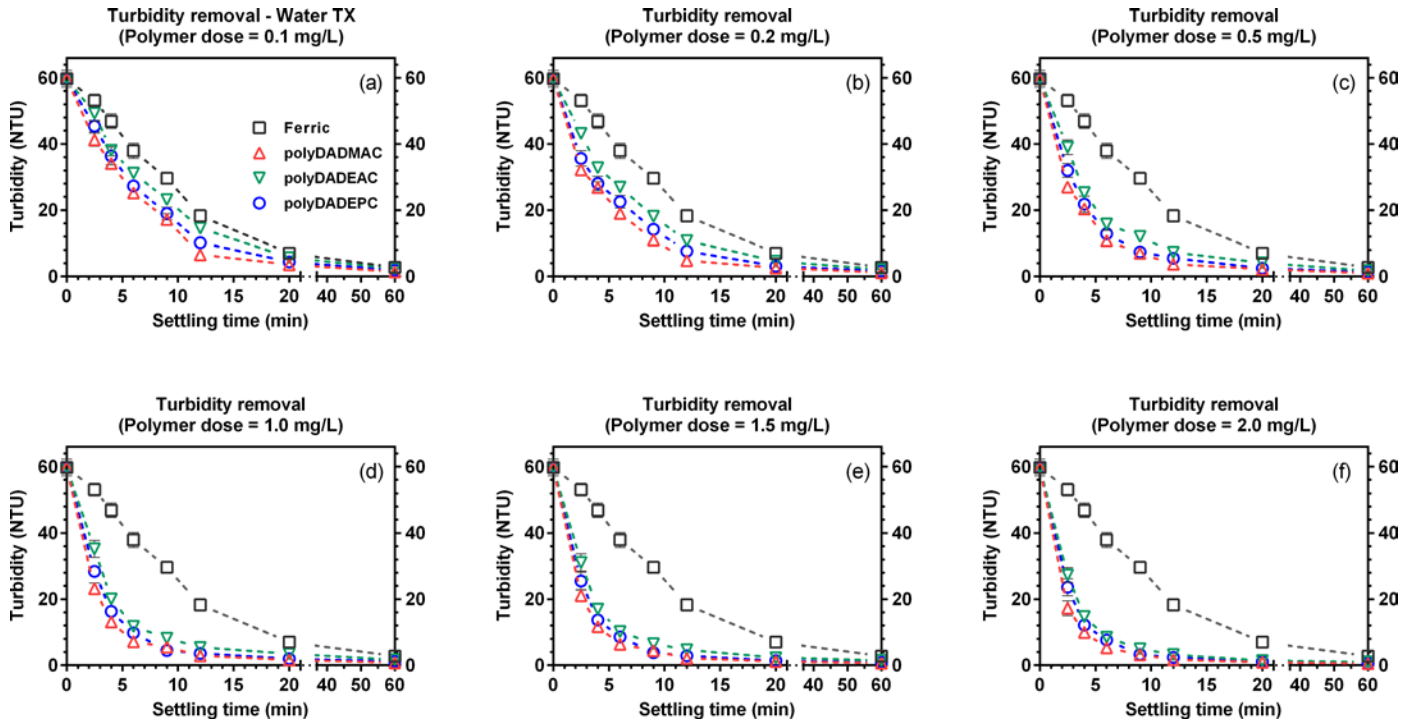

Figure S10. Time courses of turbidity removal at varying polymer doses in water TX. "Ferric" indicates that only ferric chloride was dosed to serve as a benchmark. Error bars represent the range of duplicate measurements; where absent, bars fall within symbols.

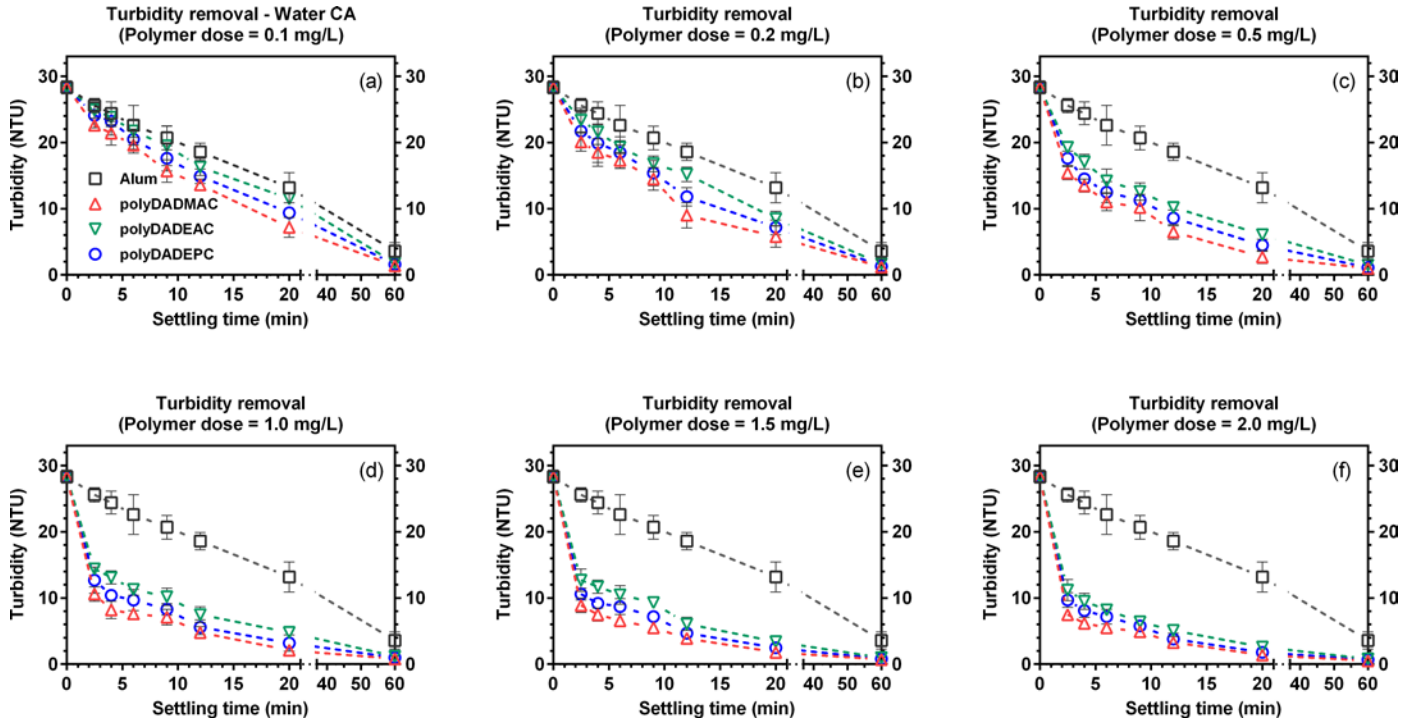

Figure S11. Time courses of turbidity removal at varying polymer doses in water CA. "Alum" indicates that only aluminum sulfate was dosed to serve as a benchmark. Error bars represent the range of duplicate measurements; where absent, bars fall within symbols.

References

1. Furman, C. S.; Margerum, D. W., Mechanism of chlorine dioxide and chlorate ion formation from the reaction of hypobromous acid and chlorite ion. *Inorg. Chem.* **1998,** *37*, 4321-4327.
2. Valentine, R. L.; Brandt, K. I.; Jafvert, C. T., A spectrophotometric study of the formation of an unidentified monochloramine decomposition product. *Water Res.* **1986,** *20*, 1067-1074.
3. Schreiber, I. M.; Mitch, W. A., Influence of the order of reagent addition on NDMA formation during chloramination. *Environ. Sci. Technol.* **2005,** *39*, 3811-3818.
4. Negi, Y.; Harada, S.; Ishizuka, O., Cyclopolymerization of diallylamine derivatives in dimethyl sulfoxide. *J. Polym. Sci., Part A-1: Polym. Chem.* **1967,** *5*, 1951-1965.
5. Le Roux, J.; Gallard, H.; Croué, J.-P., Formation of NDMA and halogenated DBPs by chloramination of tertiary amines: The influence of bromide ion. *Environ. Sci. Technol.* **2012,** *46*, 1581-1589.
6. Luh, J.; Mariñas, B. J., Bromide ion effect on *N*-nitrosodimethylamine formation by monochloramine. *Environ. Sci. Technol.* **2012,** *46*, 5085-5092.
7. Chung, Y.-L.; Olsson, J. V.; Li, R. J.; Frank, C. W.; Waymouth, R. M.; Billington, S. L.; Sattely, E. S., A renewable lignin-lactide copolymer and application in biobased composites. *ACS Sustainable Chem. Eng.* **2013,** *1*, 1231-1238.
8. Klein, A. P.; Anarat-Cappillino, G.; Sattely, E. S., Minimum set of cytochromes P450 for reconstituting the biosynthesis of camalexin, a major arabidopsis antibiotic. *Angew. Chem., Int. Ed.* **2013,** *52*, 13625-13628.
9. Terayama, H., Method of colloid titration (a new titration between polymer ions). *J. Polym. Sci.* **1952,** *8*, 243-253.
10. Kawamura, S.; Jr, G. P. H.; Shumate, K. S., Application of colloid titration technique to flocculation control. *J. Am. Water Works Assoc.* **1966,** *59*, 1003-1013.
11. Ueno, K.; Kina, K., Colloid titration-A rapid method for the determination of charged colloid. *J. Chem. Educ.* **1985,** *62*, 627.
12. Kam, S.-K.; Gregory, J., Charge determination of synthetic cationic polyelectrolytes by colloid titration. *Colloids Surf., A* **1999,** *159*, 165-179.
13. Frisch, M. J. T., G. W.; Schlegel, H. B.; Scuseria, G. E.; Robb, M. A.; Cheeseman, J. R.; Scalmani, G.; Barone, V.; Mennucci, B.; Petersson, G. A.; Nakatsuji, H.; Caricato, M.; Li, X.; Hratchian, H. P.; Izmaylov, A. F.; Bloino, J.; Zheng, G.; Sonnenberg, J. L.; Hada, M.; Ehara, M.; Toyota, K.; Fukuda, R.; Hasegawa, J.; Ishida, M.; Nakajima, T.; Honda, Y.; Kitao, O.; Nakai, H.; Vreven, T.; Montgomery, J. A., Jr.; Peralta, J. E.; Ogliaro, F.; Bearpark, M.; Heyd, J. J.; Brothers, E.; Kudin, K. N.; Staroverov, V. N.; Kobayashi, R.; Normand, J.; Raghavachari, K.; Rendell, A.; Burant, J. C.; Iyengar, S. S.; Tomasi, J.; Cossi, M.; Rega, N.; Millam, N. J.; Klene, M.; Knox, J. E.; Cross, J. B.; Bakken, V.; Adamo, C.; Jaramillo, J.; Gomperts, R.; Stratmann, R. E.; Yazyev, O.; Austin, A. J.; Cammi, R.; Pomelli, C.; Ochterski, J. W.; Martin, R. L.; Morokuma, K.; Zakrzewski, V. G.; Voth, G. A.; Salvador, P.; Dannenberg, J. J.; Dapprich, S.; Daniels, A. D.; Farkas, Ö.; Foresman, J. B.; Ortiz, J. V.; Cioslowski, J.; Fox, D. J., Gaussian 09, Revision C.01, Gaussian, Inc., Wallingford, CT. **2009**.
14. Becke, A. D., Density-functional thermochemistry. III. The role of exact exchange. *J. Chem. Phys.* **1993,** *98*, 5648-5652.
15. Lee, C.; Yang, W.; Parr, R. G., Development of the Colle-Salvetti correlation-energy formula into a functional of the electron density. *Phys. Rev. B: Condens. Matter Mater. Phys.* **1988,** *37*, 785-789.
16. Frisch, M. J.; Pople, J. A.; Binkley, J. S., Self-consistent molecular orbital methods 25. Supplementary functions for Gaussian basis sets. *J. Chem. Phys.* **1984,** *80*, 3265-3269.
17. Sun, Z.; Liu, Y. D.; Zhong, R. G., Carbon dioxide in the nitrosation of amine: Catalyst or inhibitor? *J. Phys. Chem. A* **2011,** *115*, 7753-7764.
18. Tomasi, J.; Mennucci, B.; Cammi, R., Quantum mechanical continuum solvation models. *Chem. Rev.* **2005,** *105*, 2999-3094.
19. Scuseria, G. E.; Schaefer, H. F., Is coupled cluster singles and doubles (CCSD) more computationally intensive than quadratic configuration interaction (QCISD)? *J. Chem. Phys.* **1989,** *90*, 3700-3703.

20. Ribeiro, R. F.; Marenich, A. V.; Cramer, C. J.; Truhlar, D. G., Use of solution-phase vibrational frequencies in continuum models for the free energy of solvation. *J. Phys. Chem. B* **2011,** *115*, 14556-14562.
21. Dai, N.; Mitch, W. A., Relative importance of *N*-nitrosodimethylamine compared to total *N*-nitrosamines in drinking waters. *Environ. Sci. Technol.* **2013,** *47*, 3648-3656.